Numerical Modeling of Flexible-Membrane Plate-and-Frame Filtration

Anthony D. Stickland, Ross G. de Kretser, Adam R. Kilcullen, and Peter J. Scales
Particulate Fluids Processing Centre, Dept. of Chemical and Biomolecular Engineering, The University of Melbourne, Victoria 3010, Australia

Peter Hillis
United Utilities PLC, Lingley Mere, Lingley Green Avenue, Warrington WA5 3LP, U.K.

Martin R. Tillotson
Yorkshire Water Services Ltd., Halifax Road, Bradford BD6 2LZ, U.K.

DOI 10.1002/aic.11369
Published online December 21, 2007 in Wiley InterScience (www.interscience.wiley.com).

Flexible-membrane plate-and-frame filter presses are used by many industries to dewater compressible slurries. The dewaterability of such materials is described well by compressional rheology theory. The one-dimensional numerical model of fixed-cavity plate-and-frame filtration described recently (Stickland et al. Chem Eng Sci. *2006;61:3818–3829) is extended here to include the squeeze phase employed by flexible-membrane filter presses. The model is validated by comparing full-scale plant data from an industrial waste slurry with model predictions based on the fundamental material properties of the feed slurries (measured using laboratory-based filtration tests), the operating conditions and the press dimensions. The model is then used to investigate the optimization of the throughput and final cake solids for flexible-membrane filter presses. By providing an accurate model based upon the material properties under the filtration environment seen by the material, the need for pilot-scale tests is eliminated.* © 2007 American Institute of Chemical Engineers *AIChE J,* 54: 464–474, 2008
Keywords: filtration modeling, filter optimization, waste slurries, dewatering, separations

Introduction

A wide range of industries (including minerals processing and water and wastewater treatment) use flexible-membrane plate-and-frame filter presses to dewater slurries. Such presses consist of concertinas of indented plates, which form cavities between the plates when the press is closed. The plates have flexible membranes or filter cloths mounted on the internal faces. When a pressure is applied to a suspension in the cavity, dewatering occurs and a cake forms against the membrane. The membrane separation is constant and equal to the cavity width during loading and fixed-cavity filtration, and varies when the membranes are pushed together during the air- or water-driven squeeze phase.

Plate-and-frame presses are used to recover valuable filtrate or reduce the water content in waste slurries. The performance is measured in terms of throughput and final cake solids, which depend on the press dimensions, applied pressure, membrane resistance and feed slurry material characteristics (including solids concentration, compressibility and permeability). A one-dimensional model of fixed-cavity

Current address of A. D. Stickland: ICI Wilton Applied Research Group, The Wilton Centre, Wilton, Redcar TS10 4RF, U.K.
Correspondence concerning this article should be addressed to P. J. Scales at peterjs@unimelb.edu.au.

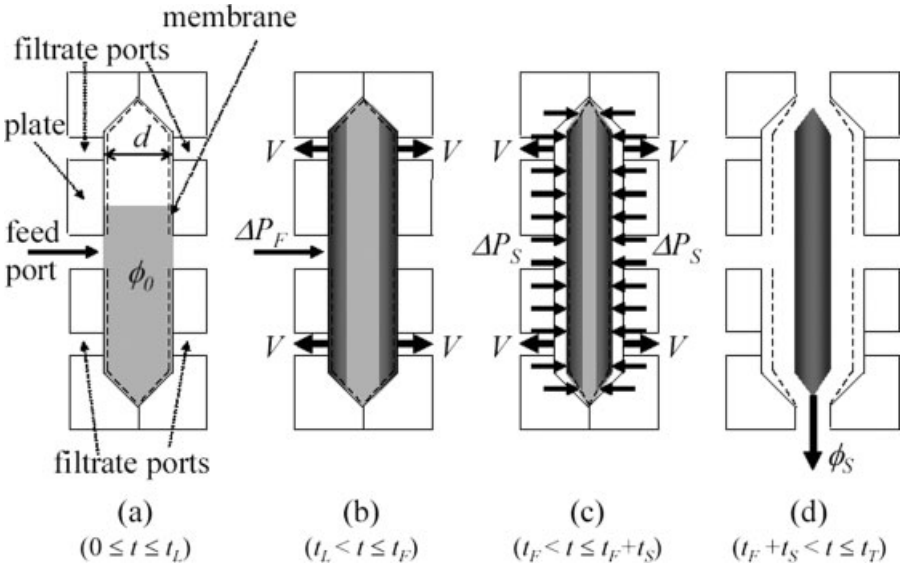

Figure 1. Flexible-membrane plate-and-frame filter press cycle.

(a) Load; (b) fixed-cavity filtration; (c) flexible-membrane filtration; and (d) unload.

filtration for compressible materials was developed in previous work,[1] based on the piston-driven filtration model of Landman et al.[2] This work extends this model to include the squeeze phase exhibited by flexible-membrane presses. The governing equation and appropriate boundary conditions are outlined, scaled to the operating conditions, and solved using a Runge-Kutta numerical method.

The flexible-membrane model is validated using onsite data from a water treatment plant (WTP) in the United Kingdom, which uses an inorganic coagulant to clarify raw water and employs a flexible-membrane press to dewater thickened slurry. Model predictions using the phenomenological material properties[3] of the feed slurries (measured using laboratory-based filtration tests[4]), the operating conditions and the press dimensions are compared with onsite results to show that the flexible-membrane model represents the appropriate filtration dynamics. The model is then used as a prediction tool to optimize the design and operation of flexible-membrane filter presses, focusing on the variation of solids throughput with cake solids for different feed concentrations, membrane resistances, applied pressures, cavity widths and handling times. This work illustrates that, if the dewatering properties of a material are known, model predictions can be made with confidence and the need for pilot-scale testing is eliminated.

Theory

The filter press cycle

The batch process of flexible-membrane plate-and-frame filtration consists of four stages, as illustrated in Figure 1. The first two stages involve loading the cavities with slurry at constant solids volume fraction, ϕ_0, for time t_L (see Figure 1a), followed by fixed-cavity filtration until time t_F (see Figure 1b) using positive displacement pumps. Slurry is fed to the cavities through central inlet ports and filtrate flows out through peripheral ports. The applied pressure during fixed-cavity filtration is ΔP_F and the time taken to reach ΔP_F is t_P. The third stage involves squeezing the membranes together using air or water pressure (ΔP_S) for time t_S (see Figure 1c). For this work, $\Delta P_S \ge \Delta P_F$ and is assumed to be instantaneous in reaching its set point and constant thereafter. Variable pressure (as a function of time or flow rate) may be incorporated but it must be monotonically increasing. At the end of the cycle, the press is opened and the filter cake (with average solids concentration, ϕ_S) is discharged (see Figure 1d). The handling time, t_H, is the time taken to open, empty and close the press, ready for the next cycle to begin. The total cycle time, t_T, is

$$t_T = t_F + t_S + t_H \tag{1}$$

Other stages such as bladder inflation or cloth washing can be incorporated within t_H, provided that the process does not affect the cake. Processes that may affect the cake, such as cake washing and cake desaturation (via vacuum or air-blow), are not considered in this work.

One-dimensional filtration

The process is simplified to one-dimension, z, with the origin at the membrane (see Figure 2). The midplane of the cavity at $h(t)$ is the other boundary, since the cavity is symmetrical. With the one-dimensional simplification, the formulation for piston-driven filtration with membrane resistance[2] can be applied to the fixed-cavity and flexible-membrane situations. The formulation for the loading and fixed-cavity filtration stages ($0 \le t \le t_F$) is detailed in previous work,[1] along with a discussion of the impact of the one-dimensional approximation. The formulation for the squeeze-phase ($t_F < t \le t_F + t_S$) of flexible-membrane presses is outlined later.

The volume of the press at maximum cavity width, V_{press}, is approximately h_0 multiplied by the total membrane area of the press, A_{press}, where h_0 is the midplane of the cavity during fixed-cavity filtration. The error arises due to the baffles

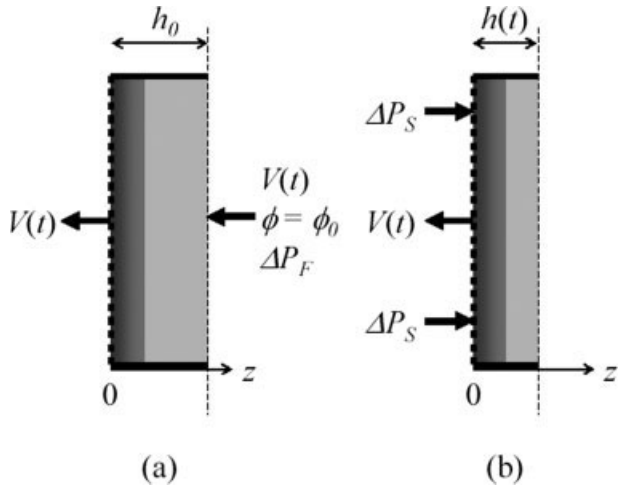

Figure 2. One-dimensional filtration.

(a) Fixed-cavity filtration and (b) flexible-membrane filtration.

used to keep the membranes apart and the feed and filtrate ports. The average suspension throughput per unit membrane area, Q, is given by the ratio of the total suspension throughput to the total time:

$$Q = \frac{V(t) + h(t)}{t_T} \tag{2}$$

$V(t)$ is the filtrate volume per unit membrane area. Q is an averaged quantity for the cycle with a maximum, Q_{max}, that depends upon the behavior of $V(t)$. The average solids throughput per unit membrane area is $\phi_0 Q$. The conservation of fluid volume during flexible membrane filtration is

$$V(t) - V_F = h_0 - h(t) \tag{3}$$

V_F is the specific filtrate volume at the end of the fixed-cavity stage. Substituting Eq. 3 into Eq. 2 gives

$$Q = \frac{V_F + h_0}{t_T} \tag{4}$$

The throughput per run ($V_F + h_0$) is unaffected by the squeeze phase, since slurry is not fed to the press during this time. In the approximation that t is proportional to V^2 during fixed-cavity filtration (which requires negligible membrane resistance, t_L and t_P to be zero and that the process remains in cake formation) and t_S is constant, Q_{max} is when t_F equals $t_H + t_S$.[5] This rule of thumb for flexible-membrane presses is useful for finding the timescale of the optimum operational regime, but is only an approximation since t is not always proportional to V^2 and t_S is a function of t_F.

Depending on the material characteristics, operating conditions, and press dimensions, Q_{max} may equal either the fixed or flexible limit. The fixed limit represents the throughput when the squeeze is not employed ($t_S = 0$) while the flexible limit represents the throughput when the squeeze begins as soon as the cavities are loaded with slurry ($t_F = t_L$). The relationship between Q_{max} and the limits and its implications are explored in detail later.

Solid–liquid separation

The phenomenological model of compressional dewatering developed by Buscall and White[3] describes flocculated suspensions as yield stress materials that dewater when the particulate network strength is exceeded. This strength is called the compressive yield stress, $P_y(\phi)$, where ϕ is the local solids volume fraction. $P_y(\phi)$ is zero at the gel point, ϕ_g, the concentration at which the network forms. The rate of dewatering is determined by the hindered settling function, $R(\phi)$, which is the hydrodynamic drag between the solid and liquid phases and is the inverse of the permeability. Assuming negligible acceleration (gravitational or centrifugal), the relevant governing equation to describe one-dimensional compressional dewatering is[3]

$$\frac{\partial \phi}{\partial t} = \frac{\partial}{\partial z}\left[D(\phi)\frac{\partial \phi}{\partial z} + \phi \frac{dV}{dt}\right] \tag{5}$$

$D(\phi)$ is the solids diffusivity, which is defined as[2]

$$D(\phi) = \frac{dP_y(\phi)}{d\phi}\frac{(1-\phi)^2}{R(\phi)} \tag{6}$$

Initial and boundary conditions

The solution of Eq. 5 requires the appropriate initial and boundary conditions. The initial conditions for the squeeze phase are given by the filtrate volume, the cavity width and the volume fraction distribution at the end of the fixed-cavity stage:

$$V(t_F) = V_F \tag{7}$$

$$h(t_F) = h_0 \tag{8}$$

$$\int_0^{h_0} \phi(z, t_F)dz = \phi_0(V_F + h_0) = \phi_F h_0 \tag{9}$$

ϕ_F is the average volume fraction at t_F. There are no more solids fed to the press; therefore, the global volumetric balance is given by a constant:

$$\int_0^{h(t)} \phi \, dz = \phi_0(V_F + h_0) \tag{10}$$

The solids pressure at the membrane, $P_y(\phi(0,t))$ (which gives $\phi(0,t)$), is the difference between ΔP_S and the pressure drop across the membrane[2]:

$$P_y(\phi(0,t)) = \Delta P_s - \eta_f R_m \frac{dV}{dt} \tag{11}$$

η_f is the fluid viscosity and R_m is the membrane resistance. The concentration gradient at the membrane, $(\partial\phi/\partial z)|_{z=0}$, is given by assuming that the membrane is impermeable to solids such that the solids velocity is zero:

$$\left.\frac{\partial \phi}{\partial z}\right|_{z=0} = -\frac{\phi(0,t)}{D(\phi(0,t))}\frac{dV}{dt} \tag{12}$$

As time gets very large, $\phi(z,t)$ approaches the compressive limit of the filter cake, $\phi_{\infty,S}$, which is given by the applied pressure:

$$P_y(\phi_{\infty,S}) = \Delta P_S \tag{13}$$

As $t \to \infty$, $V(t)$ approaches the equilibrium filtrate volume, $V_{\infty,S}$, which depends on the preceding fixed-cavity filtration:

$$V_{\infty,S} = (V_F + h_0)\left(1 - \frac{\phi_0}{\phi_{\infty,S}}\right) \tag{14}$$

Scaled equations

The problem is simplified by scaling z, $V(t)$, $h(t)$ and t to Z, $\gamma(T)$, $H(T)$ and T:

$$Z = \frac{z}{h_0} \tag{15}$$

$$\gamma(T) = \frac{V(t)}{h_0} \tag{16}$$

$$H(T) = \frac{h(t)}{h_0} \tag{17}$$

$$T = \frac{D(\phi_{\infty,S})}{h_0^2}\left(\frac{\phi_{\infty,S}}{\phi_F}\right)^2 t \tag{18}$$

Substituting these scalings into Eq. 5 gives the scaled governing equation during the squeeze phase:

$$\frac{\partial \phi}{\partial T} = \frac{\partial}{\partial Z}\left[\Delta_S(\phi)\frac{\partial \phi}{\partial Z} + \phi\frac{d\gamma}{dT}\right] \tag{19}$$

$\Delta_S(\phi)$ is the scaled diffusivity:

$$\Delta_S(\phi) = \left(\frac{\phi_F}{\phi_{\infty,S}}\right)^2 \frac{D(\phi)}{D(\phi_{\infty,S})} \tag{20}$$

The scaled conditions at T_F are

$$\begin{aligned} &\gamma(T_F) = \gamma_F \\ &H(T_F) = 1 \\ &\int_0^1 \phi(Z,T_F)\,dZ = \phi_0(\gamma_F + 1) = \phi_F \end{aligned} \tag{21}$$

Note that the time scalings for the fixed and flexible stages are based on the applied pressure and average initial volume fraction of the individual stage and are therefore different. The scaled membrane resistance during the squeeze phase, $\beta_{m,S}$, is

$$\beta_{m,S} = \frac{D(\phi_{\infty,S})}{h_0 \Delta P_S}\left(\frac{\phi_{\infty,S}}{\phi_F}\right)^2 \eta_f R_m \tag{22}$$

$\beta_{m,S}$ gives an indication of the magnitude of R_m compared to the material characteristics at the applied pressure. If $\beta_{m,S}$ is very small, R_m is negligible compared to the resistance of the filter cake and can be ignored. If $\beta_{m,S}$ is very large, the filtration dynamics are determined solely by R_m. Substituting Eq. 22 into Eq. 11 gives

$$\frac{P_y(\phi(0,T))}{\Delta P_S} = 1 - \beta_{m,S}\frac{d\gamma}{dT} \tag{23}$$

The concentration gradient at the membrane (Eq. 12) becomes

$$\left.\frac{\partial \phi}{\partial Z}\right|_{Z=0} = -\frac{\phi(0,T)}{\Delta_S(\phi(0,T))}\frac{d\gamma}{dT} \tag{24}$$

From Eq. 9, the scaled conservation during the squeeze phase is

$$\int_0^{H(T)} \phi(Z,T)\,dZ = \phi_F \tag{25}$$

An iterative solution is needed since both $\phi(0,T)$ and $(\partial\phi/\partial Z)|_{Z=0}$ are dependent upon $d\gamma/dT$, which is determined from the governing equation (Eq. 19). The iterative method is detailed later.

In the case where $\phi_0 \geq \phi_g$, the feed slurry is networked and the concentration at the top of the cake, ϕ_c, is ϕ_0. In the case where $\phi_0 < \phi_g$ and the cake has not reached the midplane during fixed-cavity filtration, an internal discontinuity at $Z_c(T)$ may exist at the boundary between the feed slurry and consolidating cake. $\phi_c = \phi_g$ while the concentration above $Z_c(T)$ is constant at ϕ_0. Equation 25 becomes

$$\int_0^{Z_c(T)} \phi(Z,T)\,dZ = \phi_0(\gamma(T) + Z_c(T)) \tag{26}$$

Numerical algorithm

The inputs to the model are the material characteristics ($P_y(\phi)$, $D(\phi)$, ϕ_g, and η_f) and the operating conditions (h_0, ϕ_0, R_m, $\Delta P(t)$, t_L, t_P, t_F, and t_S). The fixed-cavity model[1] is used to evaluate $\phi(z,t)$ and $V(t)$ up until t_F [giving V_F and $\phi(z,t_F)$]. $\phi_{\infty,S}$ and $V_{\infty,S}$ are calculated, the scalings applied and the conditions at T_F set.

An iterative Runge-Kutta numerical algorithm[6] is used to solve the squeeze-phase governing equation, subject to the appropriate boundary conditions. As with the fixed-cavity algorithm, the scaled governing equation (Eq. 19) is simplified to two coupled ordinary differential equations by introducing the scaled solids flux, $\psi(Z)$, and making a backward difference approximation in time. The concentration gradient at a particular time is

$$\frac{d\phi}{dZ} = \frac{1}{\Delta_S(\phi)}\left[\psi(Z) - \phi(Z)\frac{d\gamma}{dT}\right] \tag{27}$$

The solids flux gradient at a particular time is

$$\frac{d\psi}{dZ} = \frac{\phi(Z) - \phi^<(Z)}{\Delta T} \tag{28}$$

$\phi^<(Z)$ is the value of $\phi(Z)$ at the previous time step.

The cumulative solids volume fraction, $\Phi(Z) = \int_0^Z \phi(Z)dZ$, is used to evaluate the conservation of solids volume (the

nomenclature has changed from $Q(Z)$ in Stickland et al.[1] to avoid ambiguity):

$$\frac{d\Phi}{dZ} = \phi(Z) \tag{29}$$

For a given time step, ΔT, there is one unknown, $d\gamma^*/dT$, which is solved using an interval halving technique. The initial upper bound is given by the inverse of $\beta_{m,S}$, while the initial lower bound is zero. An estimate of γ, γ^*, is given by a first-order approximation using ΔT, $d\gamma^*/dT$ and $\gamma^<$ (the value of γ at the previous time step):

$$\gamma^* = \gamma^< + \Delta T \frac{d\gamma^*}{dT} \tag{30}$$

An estimate of H, H^*, is given by Eq. 3. Equations 27–29 are solved using fourth-order Runge-Kutta steps of ΔZ from $Z = 0$ (where $\phi(0,T)$ is given by Eq. 23 and $\psi(0,T) = \Phi(0,T) = 0$) until $\phi = \phi_c$, $Z = H^*$, or $d\phi/dZ > 0$. The accuracy of each step of ΔZ is checked using the truncation error from the fifth-order Runge-Kutta step, and ΔZ reduced if necessary. If $d\phi/dZ > 0$, $d\gamma^*/dT$ is too low and becomes the lower bound for the next iteration. If $\phi = \phi_c$ or $Z = H^*$, a test value for $\gamma(T)$, γ_{test}, is given by $\Phi(Z)$ (from Eq. 26):

$$\gamma_{test} = \frac{\Phi(Z)}{\phi_0} - Z \tag{31}$$

If $\gamma_{test} > \gamma^*$, $d\gamma^*/dT$ becomes the lower bound for the next iteration. Conversely, if $\gamma_{test} < \gamma^*$, $d\gamma^*/dT$ becomes the upper bound for the next iteration. $d\gamma^*/dT$ is iterated upon until $\gamma_{test} = \gamma^*$ to within a user-defined accuracy (10^{-8} was used here). The algorithm then proceeds to the next time step, until $T = T_S$.

In the case where $\phi_0 < \phi_g$ and the cake does not reach the midplane during fixed-cavity filtration, the transformation to $X = Z/Z_c(T)$ must be made to avoid the discontinuity at Z_c. The method outlined for fixed-cavity filtration[1] is used here with the flexible-membrane boundary conditions.

Materials and Methods

Flexible-membrane filter press results from a full-scale WTP were used to validate the model. The press dimensions were $V_{press} = 4.10$ m^3, $A_{press} = 324$ m^2, and $d = 0.032$ m ($h_0 = 0.016$ m). The difference between V_{press} and $A_{press}h_0$ arises from the size of the baffles and the feed and filtrate ports. ΔP_F was 0.6 MPa and ΔP_S was 1.0 MPa. The material was a flocculated, inorganic coagulant-rich water treatment slurry. The validation work for four runs consisted of using a constant pressure filtration device to determine the compressional properties of the feed slurry, $P_y(\phi)$, $D(\phi)$, and ϕ_0,[4,7,8] and monitoring the press performance by measuring the final average cake solids, ϕ_S, and the feed volume with time (given by the number of strokes of the positive displacement pumps and then converted to $V(t)$).

Results and Discussion

Validation results

A total of four filter press runs were analyzed, as summarized in Table 1. t_F varied from 4 to 16 h and t_S was 1 or 1.5 h. t_L and t_P were constant at 20 and 30 min, respectively. The average R_m, measured from the slope of $dt/d(V^2)$ vs. $1/V$,[7] was $(8.46 \pm 2.87) \times 10^{13}$ m^{-1}.

Table 1. Flexible-Membrane Filter Press Runs

Run	t_L (s)	t_P (s)	t_F (s)	t_S (s)	ϕ_0 (v/v)	ϕ_S (v/v)	R_m (10^{13} m^{-1})
1	1,200	1,800	56,400	3,600	0.0091	0.1219	9.61
2	1,200	1,800	46,800	3,600	0.0104	0.0993	6.20
3	1,200	1,800	39,600	4,500	0.0104	0.1042	9.79
4	1,200	1,800	15,600	4,500	0.0104	0.0946	8.25

Two feed slurries from runs 1 and 2 were characterized using stepped-pressure filtration testing. The material was flocculated and above the gel point, such that the characteristics of the individual particles were not significant. It was screened upstream to remove all large objects such as twigs and rags, and was thus assumed to be homogeneous on the length scale of the flocs. The $P_y(\phi)$ and $D(\phi)$ results, along with parameters for power-law fitting functions, were presented previously[1] as samples L1 and L2. Sample L2 was also the feed for runs 3 and 4. ϕ_S averaged 0.1050 v/v compared with $\phi_{\infty,S} = 0.1346$ v/v from extrapolations of $P_y(\phi)$ using the power-law fits, suggesting that the runs did not reach the compressive limit of the material.

The t vs. V^2 results for the four runs at the WTP are presented in Figure 3. The results for both the fixed-cavity and flexible-membrane stages are shown, since the outcomes during last stage depend on the preceding filtration. The results during fixed-cavity filtration were used to validate the fixed-cavity model.[1] After loading the press with slurry ($0 \le t \le t_L$), the transient data show an initially decreasing slope corresponding to constant flow-rate behavior because of the ramping pressure ($t_L < t \le t_P$) and the effect of R_m. A linear section follows, representing constant pressure cake formation. Toward the end of the cycle ($t \le t_F$), the results deviate from linearity, and the process enters cake compression. The fixed-cavity model shows all these characteristics, except that the onset of cake compression is predicted at a later time (not shown in Figure 3), because of the one-dimensional approximation of a feed plane rather than the reality of a feed point.[1] The errors between the results and predictions are smaller at shorter times.

To fully validate the flexible-membrane model would require measurement of $V(t)$ during the squeeze phase ($t_F < t \le t_S$), which could not be measured at the WTP utilized herein. Instead, V_S was calculated from ϕ_0, ϕ_S, h_0 and V_F using Eqs. 3 and 10 and connected to V_F by a straight line in Figure 3. Despite the lack of transient onsite data, the results and predictions show similar trends. The differences predominantly relate to the shift in V_F due to earlier than predicted compression rather than differences in the squeeze phase, although cake unevenness due to transport of material from the central feed inlet may begin to introduce errors in the squeeze phase for large t_F. The model predictions do show the transient behavior, which indicates that the process enters cake compression in some cases during flexible-membrane filtration.

The onsite results and model predictions of cake solids and throughput are given in Table 2. The model accurately

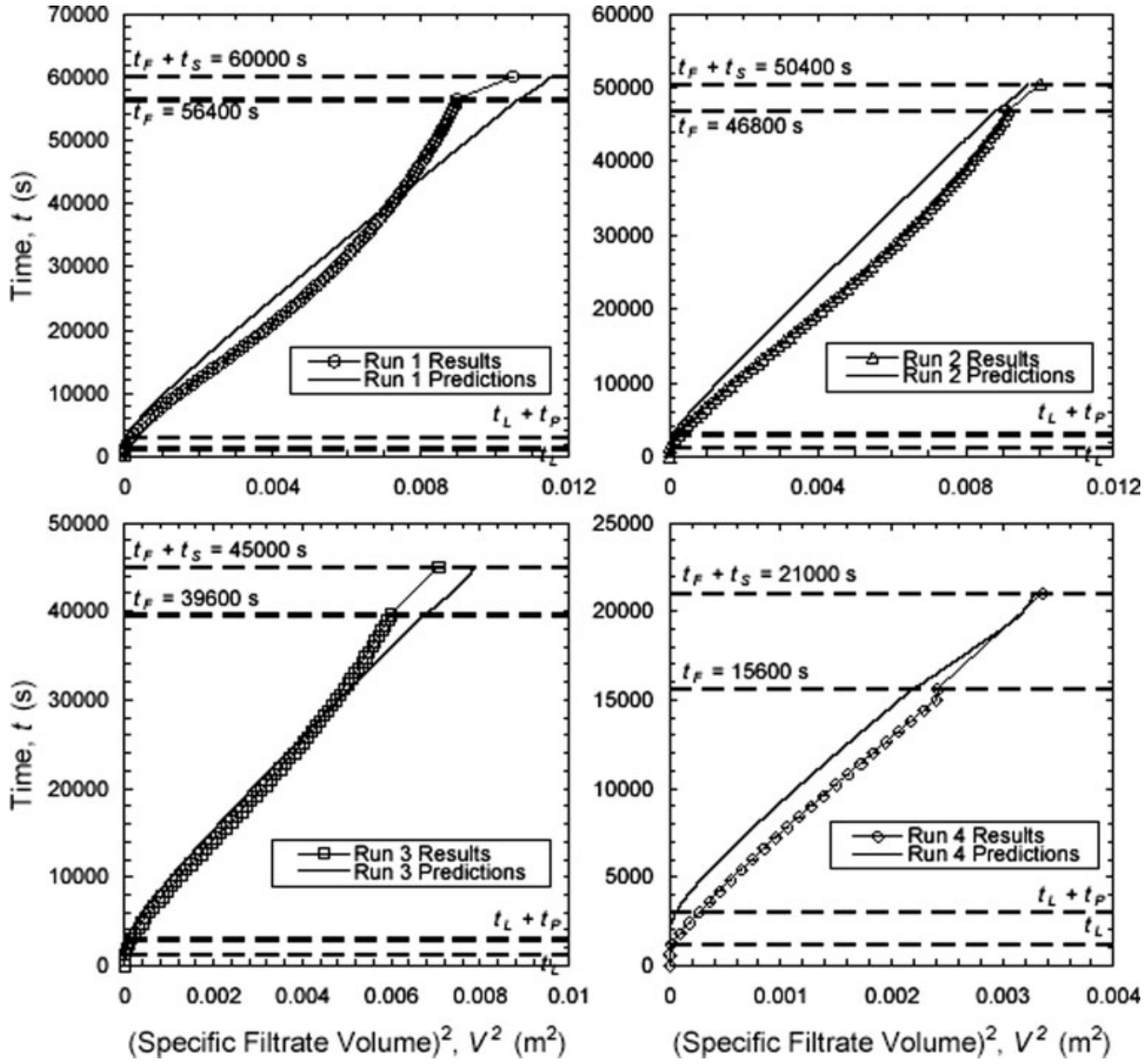

Figure 3. Transient filtrate volume results and model predictions for filter press runs 1–4.

predicts the throughput to within 7.6%, and the final solids compare well to those measured onsite, especially for runs 2 and 3. Comparisons based upon final solids are limited, since the cake varies within the cavity, although efforts were made to get representative sampling of the cake. The accuracy of the measured ϕ_S also affects the onsite calculation of Q, but to a much smaller amount. Overall, the case study at the WTP shows that by measuring the material properties in the laboratory, the model is a useful predictive tool for design and operation. For example, the effect of different flocculants, flocculation conditions and operating conditions on press performance can be predicted without relying on pilot-scale tests.

The benefits of performance optimization are illustrated by the onsite results in Table 2 without requiring any modeling—run 4, with the shortest t_F, has almost twice the throughput as run 1. As a result of this work, shorter fill times were instigated at the WTP with corresponding increases in press and plant throughput.

Flexible-membrane optimization

The flexible-membrane model was used in conjunction with the dewatering characteristics of a water treatment slurry in order to investigate the variation of throughput and final cake solids with operating conditions. In general, flexible-membrane filter presses possess greater versatility compared to fixed-cavity presses. The squeeze phase allows the press to reach any desired cake solids below $\phi_{\infty,S}$, such that t_S is a function of t_F for a given ϕ_S under specified operating conditions, compared with a set t_F to reach a given ϕ_F during fixed-cavity filtration. Figure 4a shows the squeeze time required to reach selected values of final cake solids between 0.100 and 0.175 v/v ($\phi_{\infty,S}$ for this material at 1.0 MPa is 0.1794 v/v). t_S for a given ϕ_S initially increases with t_F from the flexible limit at $t_F = t_L$ since ϕ_F is larger (that is, the average concentration at the start of the squeeze phase is greater and, therefore, the rate of filtration decreases). t_S passes through a maximum and begins to fall with longer t_F

Table 2. Onsite Measurements and Model Predictions of Final Cake Solids, ϕ_S, and Average Specific Solids Throughput, $\phi_0 Q$, for Filter Press Runs

	Onsite Results		Model Predictions		
Run	ϕ_S (v/v)	$\phi_0 Q$ (10^{-8} m/s)	ϕ_S (v/v)	$\phi_0 Q$ (10^{-8} m/s)	$\phi_0 Q$ % Diff. (%)
1	0.1219	1.583	0.0926	1.702	7.52
2	0.0993	2.152	0.0988	2.106	−2.14
3	0.1042	2.035	0.1096	2.089	2.65
4	0.0946	2.859	0.1186	2.642	−7.59

as ϕ_F nears ϕ_S, that is, the fixed-cavity stage is performing all the work. The process is at the fixed limit (that is, $t_S = 0$) when $\phi_F = \phi_S$. Note that the results for $\phi_S = 0.150$ v/v are curtailed and do not show the fixed limit, and the results for $\phi_S = 0.175$ v/v do not show the maximum in t_S.

Figure 4b shows the variation of the average solids throughput, $\phi_0 Q$ (from Eq. 4), with t_T to reach the selected values of ϕ_S. The flexible limit is at the shortest cycle time and the fixed limit is at the longest cycle time (off the scale for $\phi_S = 0.150$ and 0.175 v/v). An optimum cycle time exists when the throughput is at Q_{max}. Q is low at small t_T since t_S and t_H are large compared to t_F, and low at large t_T, since the rate of filtration during the fixed-cavity stage is continuously falling. Q decreases slightly as ϕ_S increases due to the extra squeeze time required. Despite changing ratios of t_F and t_S, the optimum time is approximately constant for the conditions presented.

The relationship between Q_{max} and the fixed and flexible limits with ϕ_S (see Figure 5) provides valuable insight into the optimization of plate-and-frame filters. Q_{max} for flexible-membrane presses approaches the throughput for fixed-cavity presses at low ϕ_S since t_S approaches zero. At high ϕ_S, t_S is large compared with t_F and Q_{max} approaches the flexible limit. At intermediate to high ϕ_S, flexible-membrane presses have greater throughputs than fixed-cavity presses, and improved cake solids are possible due to the higher pressure. This reflects the nature of fixed-cavity presses, such that both throughput and cake solids are achieved over a fixed cavity width, whereas for flexible-membrane presses, the fill-stage gives the throughput while the squeeze phase is used to achieve high cake solids.

Feed Concentration. The model was used to investigate the effect of varying the feed concentration. Figure 6a shows the squeeze time required to reach $\phi_S = 0.15$ v/v for selected values of ϕ_0 from 0.005 to 0.020 v/v. t_S at the flexible limit and at low t_F is longer as ϕ_0 increases, corresponding to greater cake solids at the beginning of the squeeze phase. This trend reverses at long times since the fixed limit (beyond the scale in Figure 6a) is reached earlier for higher ϕ_0.

Figure 6b shows $\phi_0 Q$ as a function of t_T, again illustrating the existence of an optimum cycle time when the throughput is maximized. The effect of ϕ_0 on solids throughput is very large—even though the filtration rate decreases with higher ϕ_0, the volume of solids increases. Therefore, press performance is highly dependent on the performance of prefiltration thickening or clarification. The highest solids throughput occurs when the feed concentration is maximized. However,

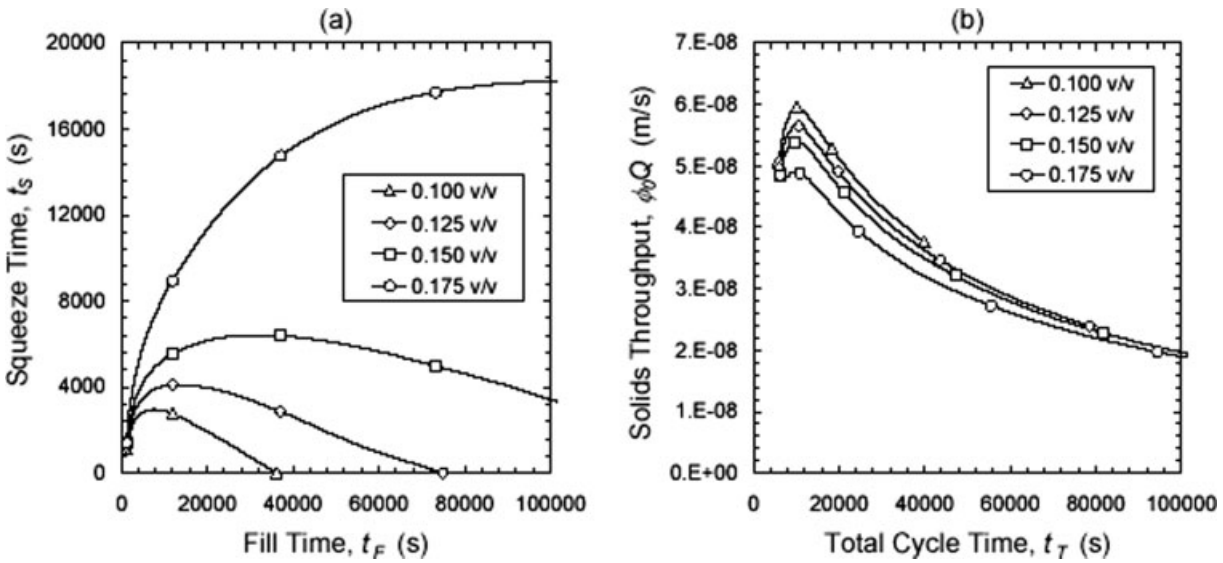

Figure 4. Model predictions for an inorganic coagulant rich water treatment slurry for $\phi_0 = 0.02$ v/v and varying final cake solids.

(a) Squeeze vs. fill time and (b) solids throughput vs. total cycle time ($\Delta P_F = 0.6$ MPa, $\Delta P_S = 1.0$ MPa, $h_0 = 0.015$ m, $t_L = 1200$ s, $t_H = 3600$ s).

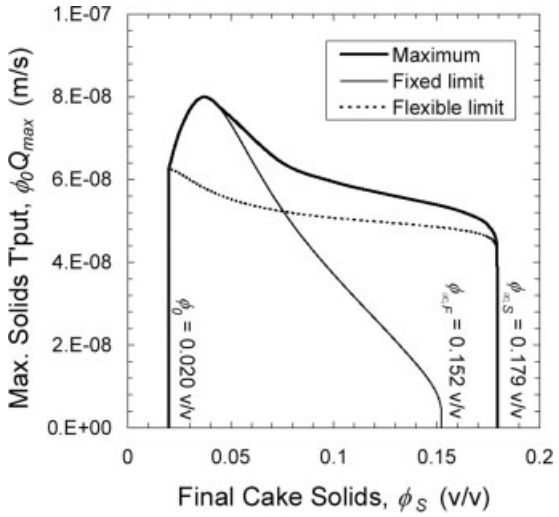

Figure 5. Model predictions of maximum solids throughput vs. final cake solids for an inorganic coagulant rich water treatment slurry (ϕ_0 = 0.02 v/v, ΔP_F = 0.6 MPa, ΔP_S = 1.0 MPa, h_0 = 0.015 m, t_L = 1200 s, t_P = 1800 s, t_H = 3600 s).

the increase with improving ϕ_0 is less than proportional to the benefit in $\phi_0 Q$—if the filtrate is valuable, Q is largest when ϕ_0 is minimized (with the caveat that thickening or clarification may be more economically feasible processes than filtration).

The model predictions for the variation of $\phi_0 Q_{max}$ with ϕ_S for a range of ϕ_0 values are shown in Figure 7, along with the fixed and flexible limiting behaviors of flexible-membrane filter presses. Q_{max} is at the fixed limit for low ϕ_S and approaches the flexible limit for high ϕ_0 and high ϕ_S. Figure 7 shows that the highest solids throughput is when the feed concentration is highest, and that the benefits of improving ϕ_0 on $\phi_0 Q_{max}$ are consistent across the ϕ_S range.

Membrane Resistance. The model was used to investigate the effects of membrane resistance. $\phi_0 Q_{max}$ is plotted in Figure 8 as a function of ϕ_S for various R_m values from 0 to 10^{15} m^{-1}. The results show that $R_m = 10^{13}$ m^{-1} has little effect on throughput, such that cleaning would be unnecessary. $R_m = 10^{14}$ m^{-1} has some effect on Q_{max}, especially at high ϕ_S where the flexible limit becomes important. R_m has a greater effect on flexible-membrane filter presses than fixed-cavity filter presses, since R_m has an influence at small times when the cake resistance is smallest. For example, at $R_m = 10^{14}$ m^{-1} and ϕ_S = 0.14 v/v, $\phi_0 Q_{max}$ is 82% of the $R_m = 0$ case, whereas the corresponding value is 90.4% for the fixed case. Therefore, cleaning may be beneficial at lower membrane resistances for flexible-membrane presses than for fixed-cavity presses. The results show that, at $R_m = 10^{15}$ m^{-1}, t_S is always so large that the press must always operate at the flexible limit, regardless of the desired cake solids.

Applied Pressure. The effect of applied pressure on average throughput was also investigated. The pressure values correspond to typical values at WTPs. Figure 9a shows the results for various fill pressures (0.6–1.0 MPa) at ΔP_S = 1.0 MPa. Increasing ΔP_F improves the fixed limit throughput and $\phi_{\infty,F}$, but the versatility of flexible-membrane presses negates this advantage at high ϕ_S. Figure 9b shows the results for various squeeze pressures (1.0–1.5 MPa) with ΔP_F = 0.6 MPa. Greater ΔP_S reduces t_S, but the reduction is small compared with t_T such that the increase in throughput is minimal. However, greater ΔP_S also increases $\phi_{\infty,S}$, such that higher final cake solids are possible. For example, ΔP_S of 1.2 MPa allows ϕ_S = 0.18 v/v whereas 1.0 MPa does not.

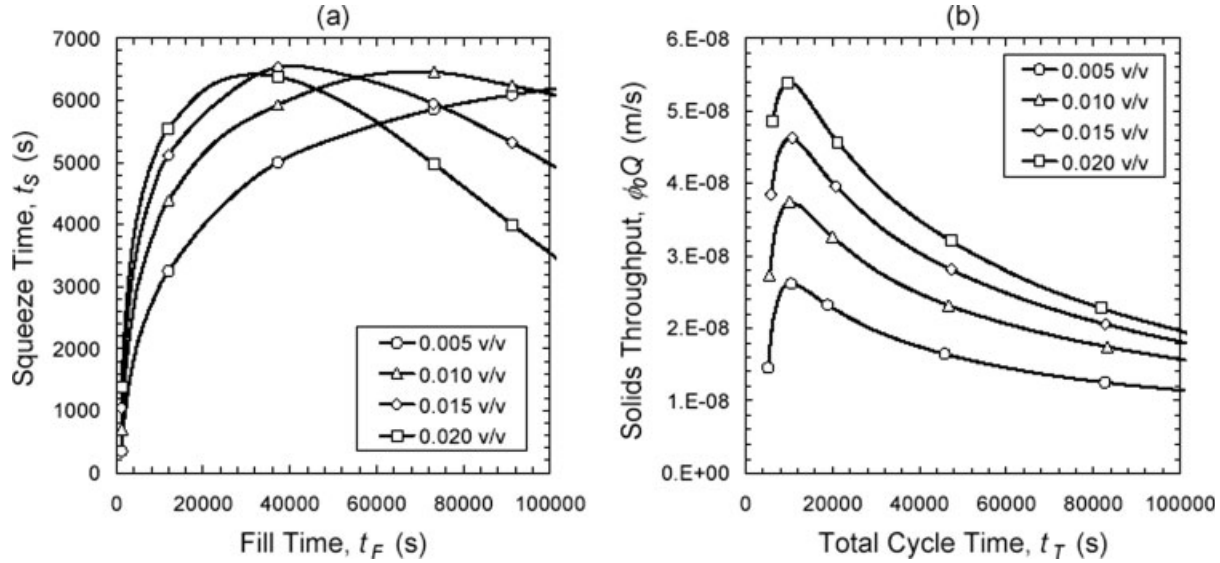

Figure 6. Model predictions for an inorganic coagulant rich water treatment slurry for varying feed concentrations and ϕ_S = 0.15 v/v.

(a) Squeeze vs. fill time and (b) solids throughput vs. total cycle time (ΔP_F = 0.6 MPa, ΔP_S = 1.0 MPa, h_0 = 0.015 m, t_L = 1200 s, t_P = 1800 s, t_H = 3600 s).

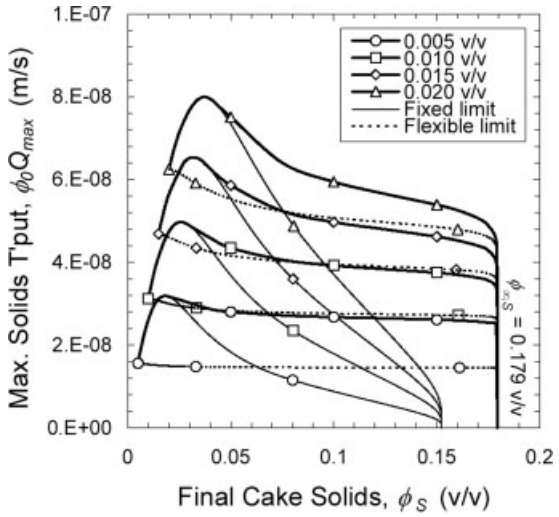

Figure 7. Model predictions of maximum solids throughput vs. final cake solids for an inorganic coagulant rich water treatment slurry at differing feed concentrations (ΔP_F = 0.6 MPa, ΔP_S = 1.0 MPa, h_0 = 0.015 m, t_L = 1200 s, t_P = 1800 s, t_H = 3600 s).

While these trends with changing applied pressure are material-specific (for example, greater ΔP_S will have little effect on $\phi_{\infty,S}$ for incompressible materials and a large effect for highly compressible materials), the model allows comparisons between the costs and benefits of changing the applied pressure if the material has been appropriately characterized. For this water treatment slurry, increasing ΔP_F has very little effect and would not be considered an option for improving filter performance. Greater ΔP_S has some effect but only at high ϕ_S, and thus would only be considered if the existing performance was nearing the compressional limit and the benefits outweighed the extra capital and operating costs.

Cavity Width. The most common cavity widths used for the filtration of water treatment slurries are about 3 cm (h_0 = 0.015 m), although some manufacturers do offer alternatives. The effect of cavity width was investigated using the model with a range of h_0 values. t_L was adjusted proportionally with h_0 to represent the reduced press volume (assuming the same number of cavities). The throughput results are presented in Figure 10. Changing h_0 from 0.005 to 0.025 m has a large effect on both the fixed and flexible limits. The fixed limit increases at low ϕ_S due to longer time spent in cake formation and decreases at high ϕ_S due to later and longer cake compression. The maximum in the fixed limit also shifts to lower ϕ_S with greater h_0. The flexible limit increases across all ϕ_S with larger h_0 due to greater initial loading, with less effect at high ϕ_S due to longer t_S.

Figure 10 shows that, despite these large changes to the limiting behaviors, varying h_0 has only a small effect on $\phi_0 Q_{max}$ for flexible-membrane presses. The smallest cavity width has the highest throughput at high ϕ_S and is subject to the fixed limit at intermediate ϕ_S. The largest cavity width has the highest throughput at low ϕ_S (at the fixed limit) and is at the flexible limit for intermediate to high ϕ_S. When not at either of the limits, increasing h_0 increases t_S, but the throughput loss is reduced by the larger initial loading. For ϕ_S from 0.10 to 0.17 v/v, the difference in throughput between cavity widths of 0.005 and 0.025 m was under 5% for the conditions examined. Thus, while cavity width has a large effect on the throughput of fixed-cavity presses, it does not necessarily impinge on flexible-membrane presses provided that the press is operating close to its maximum throughput for the given operating conditions.

Handling Time. Figure 11 shows the effect of t_H on throughput as a function of ϕ_S. Either automating the press, enhancing cake release or increasing staffing can improve t_H. Q_{max} grows with decreasing t_H since extra cycles are used and more time is spent on high rate filtration. Therefore, the shortest possible handling time is always the best. However, the optimum t_F and t_S change with t_H, such that consistent t_H is also important.

The fixed limit is affected by decreasing t_H at low ϕ_S but less at high ϕ_S, since t_H becomes a smaller proportion of t_T. The flexible limit has greater importance with decreasing t_H—as t_H is made smaller, the optimum t_F and t_S are reduced, but t_F decreases quicker such that the limit is reached where t_S is too large and Q_{max} is when t_F equals t_L.

Conclusions

This work details the theoretical development of a one-dimensional model of flexible-membrane plate-and-frame filter presses and presents a numerical algorithm to solve the governing equation. The model is capable of predicting the behavior with or without membrane resistance for networked and unnetworked feed slurries using any functional forms for the material characteristics and is able to predict cake compression during fixed-cavity filtration.

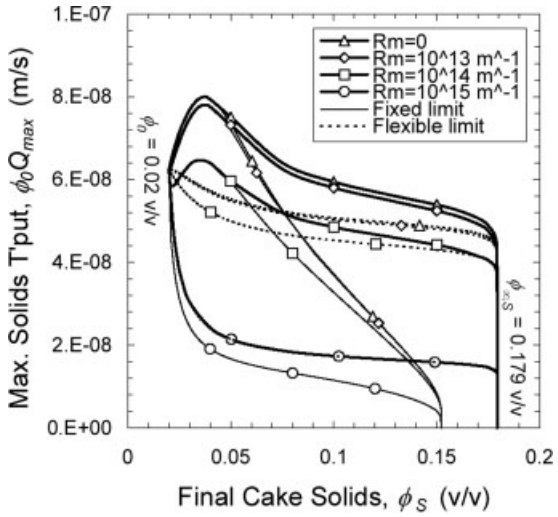

Figure 8. Model predictions of maximum solids throughput vs. final cake solids for an inorganic coagulant rich water treatment slurry with varying membrane resistance values (ΔP_F = 0.6 MPa, ΔP_S = 1.0 MPa, ϕ_0 = 0.02 v/v, h_0 = 0.015 m, t_L = 1200 s, t_P = 1800 s, t_H = 3600 s).

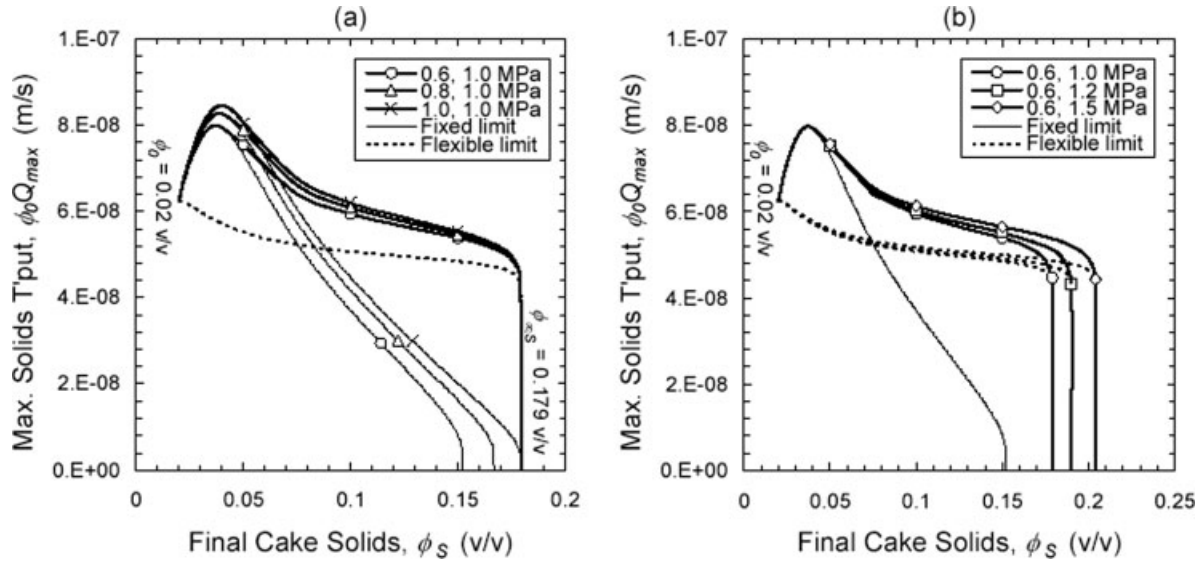

Figure 9. Model predictions of maximum solids throughput with final cake solids for an inorganic coagulant rich water treatment slurry under various pressure regimes (ΔP_F, ΔP_S) (ϕ_0 = 0.02 v/v, h_0 = 0.015 m, t_L = 1200 s, t_P = 1800 s, t_H = 3600 s).

(a) Varying fill pressure and (b) varying squeeze pressure.

The model was validated by comparing actual press performance during a case study at a WTP, with predictions based on the material characteristics of the feed slurries (measured in the laboratory), the operating conditions, and the press dimensions. Although onsite transient data during the squeeze-phase was unavailable, the model predictions for final cake solids and solids throughput showed close agreement to the measured values (within 7.6% for the throughput). The case study illustrated that, provided the material properties are measured, the model is a useful predictive tool for design and operation, providing quantification of the effects of changing materials and operating conditions and eliminating the need for pilot-scale tests.

The optimization of flexible-membrane filter presses was investigated for a coagulant-rich water treatment slurry. While the operating conditions were chosen as typical values for this material and the model results are dependent upon the material properties, the model trends are expected to be general for a wide variety of slurries. For given operating conditions, a unique combination of t_F and t_S exists to reach a desired ϕ_S at maximum throughput. This maximum is restricted at low ϕ_S by the fixed limit and at high ϕ_S by the

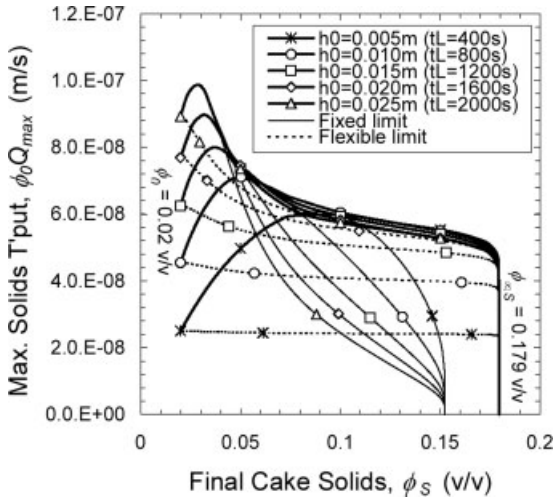

Figure 10. Model predictions of maximum solids throughput vs. final cake solids for an inorganic coagulant rich water treatment slurry with varying cavity widths (and loading times) (ΔP_F = 0.6 MPa, ΔP_S = 1.0 MPa, ϕ_0 = 0.020 v/v, t_P = 1800 s, t_H = 3600 s).

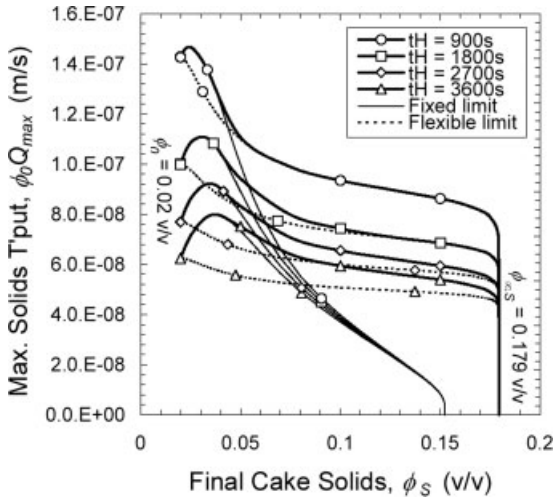

Figure 11. Model predictions of maximum solids throughput vs. final cake solids for an inorganic coagulant rich water treatment slurry with varying handling time (ΔP_F = 0.6 MPa, ΔP_S = 1.0 MPa, ϕ_0 = 0.02 v/v, h_0 = 0.015 m, t_L = 1200 s, t_P = 1800 s).

flexible limit. Depending on the material properties, press dimensions and operating conditions, the fixed limit becomes significant for incompressible materials at low ϕ_S and small h_0, while the flexible limit becomes significant for extremely compressible materials (such as wastewater slurries) at high ϕ_S, high ϕ_0, high R_m, large h_0 and small t_H.

The effect on performance of changing various operating conditions indicated that high solids throughputs are achieved when the feed concentration is highest and the handling time is minimized, providing that the operating procedures are adjusted accordingly. In contrast, high slurry throughputs are achieved when the feed concentration is lowest. For the coagulant-rich water treatment slurry, there are only small improvements with increasing applied pressure and decreasing cavity width. The inclusion of membrane resistance allows the development of cleaning protocols.

Acknowledgments

The authors acknowledge the financial support of the Particulate Fluids Processing Centre (a Special Research Centre of the Australian Research Council) and industrial sponsorship from United Utilities PLC, U.K. and Yorkshire Water Services Ltd., U.K.

Notation

A_{press} = total press membrane area (m^2)
$D(\phi)$; $\Delta_S(\phi)$ = solids diffusivity (m^2/s); scaled solids diffusivity
d = cavity width (m)
$h(t)$; $H(T)$ = feed plane position (m); scaled feed plane position
$P_y(\phi)$ = compressive yield stress (Pa)
Q = average specific throughput (m/s)
$R(\phi)$ = hindered settling function [(Pa s)/m^2]
R_m; $\beta_{m,S}$ = membrane resistance (m^{-1}); scaled membrane resistance
t; T = time (s); scaled time
$V(t)$; $\gamma(T)$ = specific filtrate volume (m^3/m^2); scaled filtrate volume
V_{press} = total press volume (m^3)
z, Z = spatial dimension (m); scaled spatial dimension
ΔP = operating pressure (Pa)
ϕ = solids volume fraction
ϕ_g = gel point solids volume fraction
$\Phi(Z)$ = cumulative solids volume fraction
η_f = fluid viscosity (Pa s)
ψ = scaled solids flux

Subscripts/superscripts

c = cake
F = fixed-cavity (fill) filtration
H = handling
L = loading
P = ramping pressure
S = flexible-membrane (squeeze) filtration
test = test value
T = total
0 = initial
∞ = equilibrium
$<$ = value at previous time step
* = estimated value

Literature Cited

1. Stickland AD, de Kretser RG, Scales PJ, Usher SP, Hillis P, Tillotson MR. Numerical modelling of fixed-cavity plate-and-frame filtration: formulation, validation and optimisation. *Chem Eng Sci*. 2006;61:3818–3829.
2. Landman KA, Sirakoff C, White LR. Dewatering of flocculated suspensions by pressure filtration. *Phys Fluids A*. 1991;3:1495–1509.
3. Buscall R, White LR. The consolidation of concentrated suspensions, Part 1: The theory of sedimentation. *J Chem Soc 1*. 1987;83:873–891.
4. de Kretser RG, Usher SP, Scales PJ, Boger DV, Landman KA. Rapid filtration measurement of dewatering design and optimisation parameters. *AIChE J*. 2001;47:1758–1769.
5. Landman KA, White LR. Predicting filtration time and maximizing throughput in a pressure filter. *AIChE J*. 1997;43:3147–3160.
6. Matthews JH. *Numerical Methods for Mathematics, Science, and Engineering*, 2nd ed. New Jersey: Prentice-Hall, 1992.
7. Usher SP, de Kretser RG, Scales PJ. Validation of a new filtration technique for dewaterability characterization. *AIChE J*. 2001;47:1561–1570.
8. Green MD, Landman KA, de Kretser RG, Boger DV. Pressure filtration technique for complete characterisation of consolidating suspensions. *Ind Eng Chem Res*. 1998;37:4152–4156.

Manuscript received May 24, 2007, revision received Aug. 29, 2007, and final revision received Oct. 19, 2007.